

Identification of Fault Characteristics in the 2021 Ambarawa Swarm Earthquake Based On Focal Mechanism Analysis

Muhammad Rizal Ramadhani ^{1,a,*}, Khafidh Nur Aziz ^{2,b}, Budiarta ²

^{1a,b} Physics, Faculty of Mathematics and Natural Sciences, Universitas Negeri Yogyakarta, Karang Malang, Sleman, Daerah Istimewa Yogyakarta 55281, Indonesia

² Badan Meteorologi, Klimatologi, dan Geofisika (BMKG), Balecatuur, Sleman, Daerah Istimewa Yogyakarta 55294, Indonesia

e-mail: ^a muhammadrizal.2020@student.uny.ac.id, ^b khafidh.na@uny.ac.id, and ^c budiarta@bmgk.go.id

* Corresponding Author

Received: 14 December 2024; Revised: 20 June 2025; Accepted: 30 December 2025

Abstract

Swarm earthquakes occur repeatedly within a certain time frame and occur in the same location with small earthquake strengths. A swarm earthquake occurred in the Ambarawa region of Central Java from October to November 2021. This research aims to determine the characteristics of new faults and the causes of fault activity in the 2021 Ambarawa earthquake. The method used in determining the characteristics of faults that cause swarm earthquakes is P wave first motion polarity recorded by the seismograph. A total of 7 earthquake data were analyzed using the P-wave first motion polarity method which produced compression/dilation data, azimuthal angle, and take-off angle. Analysis of the focal mechanism using compression/dilatation data, azimuthal angle, and take-off angle produces strike, dip, and rake values. The strike value in the focal mechanism of the 2021 Ambarawa earthquake ranges from N 54°, N 69°, N 168° to N 208°, and N 292°. The dip value in the focal mechanism of the 2021 Ambarawa earthquake has a value of 40° to 88°. The rake value in the focal mechanism of the 2021 Ambarawa earthquake has a negative value, indicating that it is a type of normal fault. The characteristics of the cause of the earthquake are caused by local faults in the Telomoyo Volcano area with normal fault types and shear faults. Local fault activity is indicated by the local pressure on the geothermal reservoir that flows magma fluid from the reservoir to the surface.

Keywords: Focal Mechanism, Swarm Earthquake, Fault, Ambarawa

How to cite: Ramadhani M R, Aziz K N, Budiarta. Identification of Fault Characteristics in the 2021 Ambarawa Swarm Earthquake Based On Focal Mechanism Analysis. *Jurnal Penelitian Fisika dan Aplikasinya (JPFA)*. 2025; 15(1): 71-83. DOI: <https://doi.org/10.26740/jpfa.v15n2.p1-12>.

© 2024 Jurnal Penelitian Fisika dan Aplikasinya (JPFA). This work is licensed under [CC BY-NC 4.0](https://creativecommons.org/licenses/by-nc/4.0/)

INTRODUCTION

Swarm earthquakes generally consist of small-magnitude earthquakes [1]. Several areas in Indonesia have experienced swarm earthquakes, namely around Sinabung Volcano in 2010-2013 [2], West Halmahera in 2015-2016 [3], around Bekancan Area in 2015-2017 [4], Jailolo Volcano in 2015-2016 [5], and Salak Volcano in 2019 [6]. Swarm earthquakes are characterized by an increased earthquake occurrence rate in a particular region [7]. Swarm earthquakes predominantly occur in areas around volcanoes [8,9]. The cause of swarm earthquakes can be attributed to volcanic eruptions or the presence of geothermal energy in the area around the volcano [10-13].

A swarm earthquake occurred in the Ambarawa region of Central Java from October to November 2021 [14]. The Ambarawa geological conditions are located near the Rawapening Lake, Telomoyo Volcano, and Ungaran Volcano [15]. Telomoyo volcanoes and Ungaran volcanoes are inactive volcanoes with geothermal energy potential [16-19]. The Rawapening Lake was formed by the Rawapening fault activity [20]. Swarm earthquakes that occur in Ambarawa have epicentres around the Rawapening lake and the Telomoyo Volcano areas [14]. Knowledge of the causes of swarm earthquakes can be determined by knowing earthquake characteristics [21]. The earthquake characteristics can be analyzed using focal mechanisms [22-24]. Solution focal mechanism analysis can be performed using several methods, namely the tensor moment method [25-26] and P-wave first-motion polarities [27-28].

Previous research conducted by Supendi [14], explained that the swarm earthquake was caused by the presence of new fault activity in the Ambarawa region. Another research conducted by Abdullah [29], explained that the swarm earthquake was also caused by the presence of a new fault that had a strike value to the northwest-southeast and a dip value of 90. However, these studies have not yet explained the characteristics of the fault that caused the Ambarawa earthquake using focal mechanism analysis and the lack of information regarding the causes of fault activity in the Ambarawa region. Therefore, the author conducted a study on the characteristics of swarm earthquakes in the Ambarawa region using the P-wave first-motion polarity method and focal mechanism analysis. The author has the following objectives in this study, among others to determine the characteristics of the faults that caused earthquakes in the Ambarawa region in 2021 based on focal mechanism analysis and to determine the causes of fault activity in earthquakes that occurred in the Ambarawa region in 2021. This study still has several spatial aspects, namely the absence of direct observations related to the faults that cause earthquakes and the identification of the characteristics of the earthquakes analyzed is still done manually.

METHOD

Source Data

The data used in this study are 96 data points from the BMKG Sleman Geophysical Station. The data includes the original time, arrival time, longitude, latitude, magnitude, and depth of the earthquake. The earthquake data analyzed are earthquake data with a strength of less than magnitude 4. The direction of the initial movement of the P wave, the recording station, the azimuth angle, and the take-off angle are the data to be analyzed.

Focal Mechanism

The focal mechanism used in this study is the P-wave first motion polarity method. The analysis of the focal mechanism is conducted using manual stereographic projection. This aims to facilitate the determination of the fault plane due to the earthquake's small magnitude.

P-wave first motion polarity

The amplitude distribution of P waves, A_P , for a point source exhibiting a purely double-couple shear mechanism is characterized within a spherical coordinate system (θ, φ) [30].

$$A_P(\theta, \varphi) = \cos \varphi \sin 2\theta \quad (1)$$

This equation segments the focal sphere into four distinct quadrants. For a seismic point source, the focal sphere is centered around the source and has a negligibly small radius [31]. Within each

quadrant, the P-wave first motion (polarity) remains constant, while the amplitudes are significant toward the center of the quadrant and diminish (or become zero) closer to (or directly at) the fault plane and the auxiliary plane, which is oriented perpendicularly to the fault plane [32-33].

The determination of fault planes can be achieved through the analysis of P-wave first motion polarities, particularly in the case of smaller earthquakes [34-35]. By examining the P-wave first motion polarities, it is possible to develop quantifiable polarity graphs on a Wulff equal-angle net or a Lambert-Schmidt equal area projection. However, this method takes a long time and has a fairly low level of accuracy if it does not use deep learning [27-28].

This section describes the ideal division of quadrants exhibiting positive and negative polarities. The quadrants are separated by two fault planes, which are considered to be in a uniform full space and perpendicular to each other [36]. Ultimately, this process yields either a black-and-white quadrant or a quadrant tinted in various colors, as represented by a horizontal 2D focal sphere, commonly known as the "beach ball" solution. The beach ball is then plotted and presented with respective figures for the strike, dip, and rake of both fault planes.

Beach Ball

Begin by preparing a sheet of transparent paper with a needle positioned at the center of the grid, and label the directions North, East, South, and West, as well as the grid edges, using stereographic projection paper for assistance. Then, all data points are transferred onto the transparent paper based on the azimuth values, take-off angle values, and the P-wave first motion polarity. The polarity of each point is indicated as – for dilation and + for compression [37].

As a first step, prepare a sheet of transparent paper with a needle at the center of the grid and mark the directions North, East, South, and West, as well as the grid boundaries on the transparent paper using the aid of stereographic projection paper. Next, all data points are transferred according to the azimuth values, take off angle values, and the P-wave first motion polarity on the transparent paper [30]. The polarity of each is marked as – for dilation and + for compression. Then, the transparent paper should be rotated over the center of the grid until a great circle meridian on the underlying grid that separates the + and – marks is found [38]. With a clockwise rotation, a demonstration of a meridian that effectively separates the first compression motion from the dilatation motion can be found on the left side [39]. The trace of this great circle should be drawn with a marker on the transparent paper and referred to as fault plane one = FP1.

Next, find the trace of the second (or auxiliary) fault plane FP2, which is located 90° apart from FP1. Therefore, the pole P1 of FP1, which FP2 must pass through, must be marked on the transparent sheet [38]. P1 is perpendicular to the center of FP1, 90° away to the right [30]. Another large circle can be found by rotating the transparent sheet counterclockwise, which passes through P1 and separates at least most of the black points from most of the open circle on the right side [38]. FP1 and FP2 intersect at the bottom of the grid at a 90° angle. Thus, the pole P2 of FP2 will be placed on FP1, 90° above the intersection point of these two fault planes. Note that all angles must be measured on the large circle [30].

RESULTS AND DISCUSSION

The earthquake that occurred in the Ambarawa area was an earthquake that did not have a main earthquake with a magnitude of 1.9 to 3.5 and a depth of less than 15 km. An earthquake that does not have a main earthquake within a certain time span is called a swarm earthquake [40]. The

earthquake epicenters were distributed on land and in the vicinity of Telomoyo Volcano [41], particularly in the western to northeastern parts of Telomoyo Volcano and the coast of Lake Rawa Pening (Figure 1). The distribution of the 2021 Ambarawa earthquake has an earthquake strength of magnitude 1.9 to 3.5 with a depth of less than 15 km. This depth is included in the shallow earthquake type (<60 km) [42]. Based on their depth, earthquakes that occur at shallow depths are generally caused by fault activity [43-44]. The epicenter of the earthquake was located close to regional faults, namely the Merapi-Merbabu Fault in the east-south and the Rawapening Fault in the northeast part of the epicenter. This indicates that the Ambarawa earthquake may have been caused by local fault activity in the area.

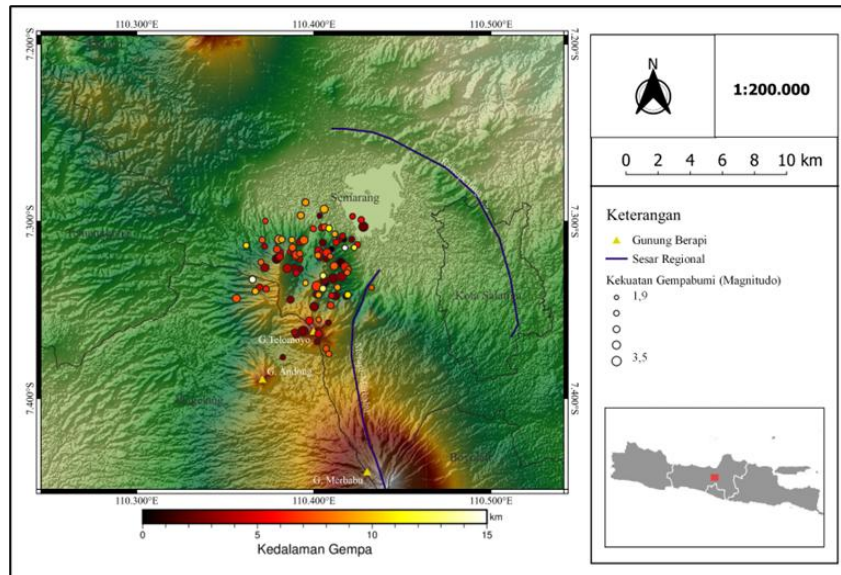


Figure 1. Map of the distribution of the epicenters of the Ambarawa 2021 swarm earthquake. The epicentral distribution of swarm earthquakes is located at the coordinates 110.3562° east - 110.4326° east and 7.28928° north - 7.37667° south.

The fault plane that caused the swarm earthquake that occurred in the Ambarawa Region in 2021 can be identified by looking at the concentration of the distribution of the location and depth of the hypocenter through cross-section lines [45]. The cross section shows a cluster of earthquakes displaced from different layers to a particular location in the sedimentary layer (Figure. 2). The results of cross-sections AB and CD form a clustering pattern (Figure. 3). The pattern seen in the cross-section results indicates that the same source caused the 2021 Ambarawa swarm earthquake. The pattern or cluster is believed to be in the geothermal manifestation area north of Telomoyo Volcano [46]. Geothermal reservoirs in the Telomoyo Volcano region are located at depths of 1500 m to 3000 m [47-48]. Geothermal reservoirs can be found at depths of 2000 m [49-50]. The author indicates that based on the depth of the 2021 Ambarawa earthquake, it can be suspected that it is related to fluid activity in the geothermal reservoir which is the source of the earthquake.

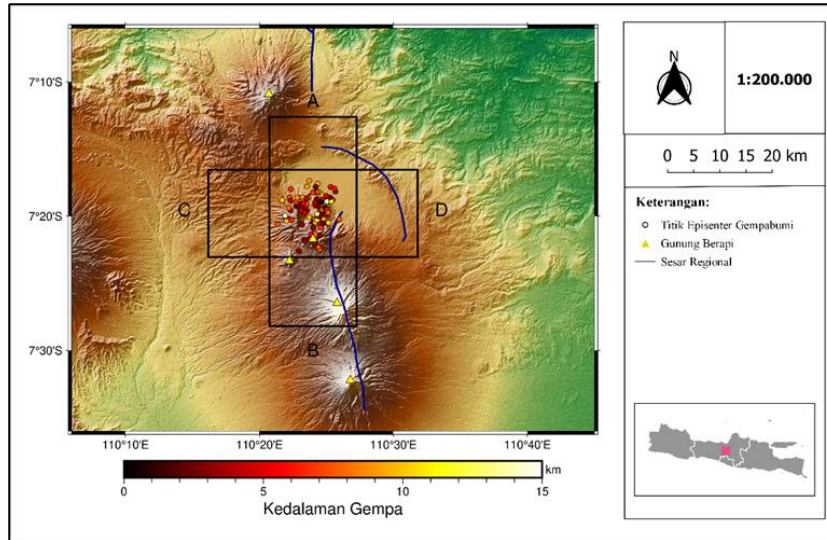


Figure 2. Cross section of the 2021 Ambarawa swarm earthquake. AB cross-section is located at coordinates 7.19° N and 110.40° E to 7.51° N and 110.40° East. The CD cross-section is located at coordinates 7.325°N and 110.24°E to 7.325°N and 110.56°E. The length of the AB and CD cross sections is 33 km with a scale of 5 km.

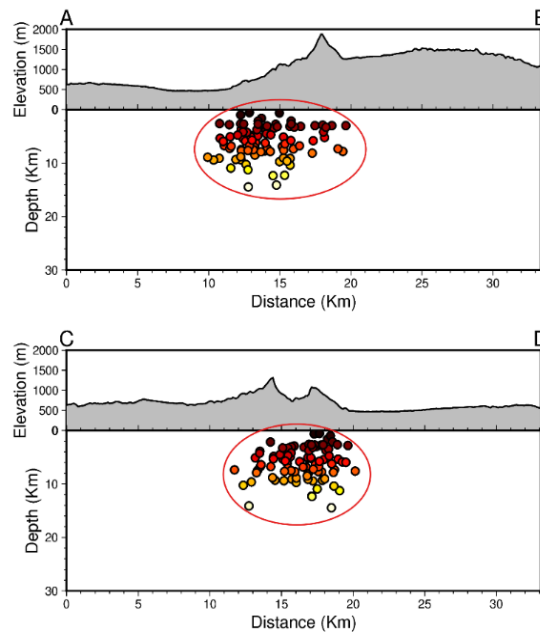


Figure 3. Cross-sectional results of the 2021 Ambarawa swarm earthquake. The epicenter of the Ambarawa swarm earthquake in 2021 is at a depth of less than 15 km and is in the vicinity of Telomoyo Volcano

The focal mechanism solution for the 2021 Ambarawa earthquake has strike slip-normal fault, normal-strike slip fault and normal fault types (Figure 4). The distribution of focal mechanisms in the 2021 Ambarawa earthquake was in the north, northwest and west of Telomoyo Volcano (Figure 5). 5 out of 7 focal mechanism solutions have strike slip-normal fault types with magnitudes ML3.1, ML3.3 at 03:45:14 and 23:52:05, ML3.4, and ML3.5. Structural and kinematic data indicate that

common geothermal fluid pathways correspond to normal to oblique strike-slip faults [51-52].

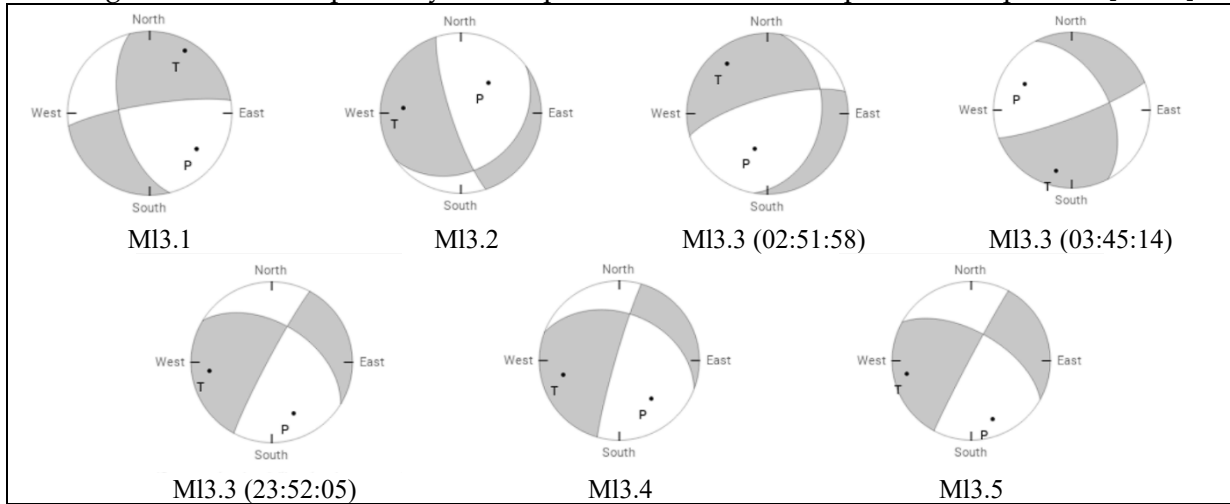


Figure 4. Focal mechanism solution for the 2021 Ambarawa swarm earthquake. The focal mechanism solution for the magnitude ML3.1 earthquake has a strike slip-normal fault type with a rightward sliding direction or dextral strike slip-normal fault with a fault plane direction of $N 261^\circ$. Focal mechanism solution at earthquake magnitude ML3.3 (03:45:14), ML3. 3 (23:52:05), ML3.4, ML3.5 have strike slip-normal fault type with leftward shear direction or sinistral strike slip-normal fault with fault plane direction of $N 69^\circ$ for focal mechanism ML3.3 (03:45:14), $N 208^\circ$ for focal mechanism ML3.3 (23:52:05), $N 196^\circ$ for focal mechanism ML3.4, and $N 208^\circ$ for focal mechanism ML3.5. The ML3.2 focal mechanism solution has a normal fault type with a fault plane direction of $N 162^\circ$. Focal mechanism solution ML3,3 (02:51:58) has a normal-sinistral strike slip fault type with a fault plane direction of $N 254^\circ$.

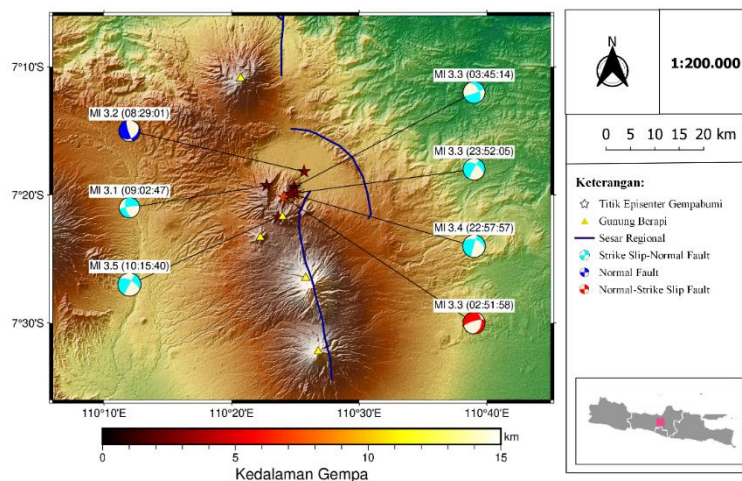


Figure 5. Distribution of focal mechanisms of the 2021 Ambarawa earthquake. The distribution of focal mechanisms aims to see patterns or similarities between focal mechanism solutions.

The direction of the fault plane in the focal mechanism of the 2021 Ambarawa swarm earthquake tends to have strike values of $N 168^\circ$ to $N 292^\circ$, $N 54^\circ$ and $N 69^\circ$. The dip value in the *Muhammad Rizal Ranadhani, et al*

strike-slip faults. These fault patterns are often observed in geothermal areas [21,58-59]. Normal faults are generally found in rift zones where tensile stresses dominate [8,21]. These layers are often highly permeable, providing vertical pathways for convective circulation. Strike-slip faults have dextral or sinistral movement forming pull-apart basins, which will create a path for geothermal fluid flow [11,31].

Geothermal areas in the Telomoyo Volcano region, as evidenced by the presence of geothermal reservoirs and local faults that control geothermal fluids, can be one of the causes of earthquakes that occur in the Ambarawa area, especially in the area around Telomoyo Volcano [54-55]. The long earthquake period is thought to be caused by excessive and continuous fluid transport from the reservoir to the surface/shallow depth through local faults/faults or stress changes due to an increase in hot material that can cause rock deformation in the weak zone around the geothermal reservoir [54, 56-57]. Stress changes due to an increase in hot material in the geothermal region caused by local fault activity can trigger swarm earthquakes within a certain period of time [58-60].

This research has novelty compared to previous studies that have not yet explained the characteristics of the faults causing the 2021 Ambarawa swarm earthquake. However, this study still has shortcomings in various aspects, namely the absence of direct observation which is a deficiency in this study. In addition, the method used in determining the focal mechanism still uses a manual method and does not use the latest model. With this study, it is hoped that there will be other studies on the 2021 Ambarawa swarm earthquake using direct observation or using more efficient and latest methods.

CONCLUSION

It discusses the characteristics of the causes of the 2021 Ambarawa swarm earthquake. The epicenter of the swarm earthquake is around Telomoyo Volcano which has geothermal energy potential. The P-wave first motion polarity method is used to determine the characteristics of the fault that causes the earthquake. The results of this study explain that the characteristics of the cause of the earthquake are caused by local faults in the Telomoyo Volcano area with normal fault types and strike-slip faults. The activity of local faults is indicated by local pressure on the geothermal reservoir that flows magma fluid from the reservoir to the surface.

REFERENCES

- [1] D. R. Shelly, "Examining the Connections Between Earthquake Swarms, Crustal Fluids, and Large Earthquakes in the Context of the 2020–2024 Noto Peninsula, Japan, Earthquake Sequence," *Geophys Res Lett*, vol. 51, no. 4, Feb. 2024, doi: <https://10.1029/2023GL107897>.
- [2] V. L. Ipmawan, M. Iguchi, T. Ohkura, T. Tameguri, and H. Triastuty, "Magma intrusion process during pre-magmatic period (2010–2013) of Sinabung volcano as revealed by seismicity of volcano-tectonic and hybrid earthquakes," *Journal of Volcanology and Geothermal Research*, vol. 450, p. 108078, Jun. 2024, doi: <https://10.1016/j.jvolgeores.2024.108078>.
- [3] A. Dian Nugraha *et al.*, "Hypocenter Relocation of Earthquake Swarm in West Halmahera, North Molucca Region, Indonesia by using Double-Difference Method and 3D Seismic Velocity Structure," *IOP Conf Ser Earth Environ Sci*, vol. 62, p. 012053, Apr. 2017, doi: <https://10.1088/1755-1315/62/1/012053>.
- [4] A. D. Nugraha, P. Supendi, S. Widiyantoro, Daryono, and S. Wiyono, "Earthquake swarm analysis around Bekancan area, North Sumatra, Indonesia using the BMKG network data: Time periods of

February 29, 2015 to July 10, 2017," 2018, p. 020092. doi: <https://doi.org/10.1063/1.5047377>.

- [5] A. P. Astuti, N. S. Arifuddin, M. I. Tahir, E. M. Elsera, and M. F. I. Massinai, "Characteristic of 27th September – 7th October 2017 earthquake swarms in Jailolo Volcano, West Halmahera, Indonesia, based on hypocenter and b-value," *IOP Conf Ser Earth Environ Sci*, vol. 851, no. 1, p. 012004, Oct. 2021, doi: <https://doi.org/10.1088/1755-1315/851/1/012004>.
- [6] P. Supendi *et al.*, "Earthquake Swarm Analysis around Mt. Salak, West Java, Indonesia, Using BMKG Data from August 10 to November 24, 2019," *IOP Conf Ser Earth Environ Sci*, vol. 873, no. 1, p. 012002, Oct. 2021, doi: <https://doi.org/10.1088/1755-1315/873/1/012002>.
- [7] D. Essing and P. Poli, "Unraveling Earthquake Clusters Composing the 2014 Alto Tiberina Earthquake Swarm via Unsupervised Learning," *J Geophys Res Solid Earth*, vol. 129, no. 1, Jan. 2024, doi: <https://doi.org/10.1029/2022JB026237>.
- [8] M. Mesimeri, L. Passarelli, S. Cesca, F. Maccaferri, and F. Lanza, "Editorial: Earthquake swarms and complex seismic sequences in tectonic and volcanic areas," *Front Earth Sci (Lausanne)*, vol. 11, Oct. 2023, doi: <https://doi.org/10.3389/feart.2023.1295920>.
- [9] E. Aydar, C. Diker, İ. Ulusoy, and E. Şen, "Volcanic unrest possibilities in response to recent Obruk seismic swarm on and around Hasandağ stratovolcano (Central Anatolia, Turkey)," *Comptes Rendus. Géoscience*, vol. 353, no. 1, pp. 1–18, Mar. 2021, doi: <https://doi.org/10.5802/crgeos.46>.
- [10] M. Pola, M. Cacace, P. Fabbri, L. Piccinini, D. Zampieri, and F. Torresan, "Fault Control on a Thermal Anomaly: Conceptual and Numerical Modeling of a Low-Temperature Geothermal System in the Southern Alps Foreland Basin (NE Italy)," *J Geophys Res Solid Earth*, vol. 125, no. 5, May 2020, doi: <https://doi.org/10.1029/2019JB017394>.
- [11] M. Zucchi, "Faults controlling geothermal fluid flow in low permeability rock volumes: An example from the exhumed geothermal system of eastern Elba Island (northern Tyrrhenian Sea, Italy)," *Geothermics*, vol. 85, p. 101765, May 2020, doi: <https://doi.org/10.1016/j.geothermics.2019.101765>.
- [12] I. Koulakov, V. Komzeleva, S. Z. Smirnov, and S. B. Bortnikova, "Magma-Fluid Interactions Beneath Akutan Volcano in the Aleutian Arc Based on the Results of Local Earthquake Tomography," *J Geophys Res Solid Earth*, vol. 126, no. 3, Mar. 2021, doi: <https://doi.org/10.1029/2020JB021192>.
- [13] T. J. Jones, C. D. Reynolds, and S. C. Boothroyd, "Fluid dynamic induced break-up during volcanic eruptions," *Nat Commun*, vol. 10, no. 1, p. 3828, Aug. 2019, doi: <https://doi.org/10.1038/s41467-019-11750-4>.
- [14] P. Supendi *et al.*, "Analysis of the Banyubiru Ambarawa-Salatiga Earthquake Swarm, Central Java, October 23 - November 5, 2021," *Not Published*, pp. 1–6, 2021, Accessed: Dec. 11, 2024. [Online]. Available: <https://www.bmkg.go.id/artikel/?p=analisis-gempabumi-swarm-banyubiru-ambarawa-salatiga-jawa-tengah-tanggal-23-oktober-5-november-2021&lang=ID>
- [15] A. V. Amalia *et al.*, "KONDISI LINGKUNGAN DANAU RAWA PENING," *Bookchapter Alam Universitas Negeri Semarang*, no. 3, pp. 123–148, Jun. 2023, doi: <https://doi.org/10.15294/ka.v1i3.152>.
- [16] B. Setiyono *et al.*, "Considering Social Aspects of Geothermal Project: The Case of Social Mapping of Geothermal Project on Mount Ungaran," *E3S Web of Conferences*, vol. 125, p. 10009, Oct. 2019, doi: <https://doi.org/10.1051/e3sconf/201912510009>.
- [17] J. Marin, A. Paskarana, E. B. S. Sandy, and J. Agustian, "Assessing Geotourism Aspects of Ungaran Geothermal Areas for Promoting Sustainable Energy through Volcano-Geothermal Tourist Destination," *IOP Conf Ser Earth Environ Sci*, vol. 1245, no. 1, p. 012018, Sep. 2023, doi: <https://doi.org/10.1088/1755-1315/1245/1/012018>.
- [18] Y. Z. Abdillah *et al.*, "Geochemistry of Cold Springs in Geothermal Exploration Stage – Case Study of Candi Umbul Telomoyo, Central Java," *IOP Conf Ser Earth Environ Sci*, vol. 1293, no. 1, p. 012004,

Jan. 2024, doi: <https://10.1088/1755-1315/1293/1/012004>.

- [19] G. Yuliyanto and T. Yulianto, "Microtremor data and HVSR method of geothermal manifestation of Mt. Telomoyo, Central Java, Indonesia," *Data Brief*, vol. 51, p. 109721, Dec. 2023, doi: <https://10.1016/j.dib.2023.109721>.
- [20] W. Partono, M. Irsyam, and S. P. Retno Wardani, "Development of seismic risk microzonation map for Semarang due to Semarang fault earthquake scenarios with maximum magnitude 6.9 Mw," *MATEC Web of Conferences*, vol. 159, p. 01011, Apr. 2018, doi: <https://10.1051/mateconf/201815901011>.
- [21] V. Sharma, D. Kumar, B. Sharma, and P. Chingtham, "Characteristics of earthquake swarm activity observed in the Palghar region of Indian Peninsula from January 2019 to October 2020," *Quaternary Science Advances*, vol. 12, p. 100099, Oct. 2023, doi: <https://10.1016/j.qsa.2023.100099>.
- [22] Y. Cheng, E. Hauksson, and Y. Ben-Zion, "Refined Earthquake Focal Mechanism Catalog for Southern California Derived With Deep Learning Algorithms," *J Geophys Res Solid Earth*, vol. 128, no. 2, Feb. 2023, doi: <https://10.1029/2022JB025975>.
- [23] Abhishek, M. Sandhu, B. Sharma, D. Kumar, R. B. S. Yadav, and S. S. Teotia, "Source characteristics of earthquakes in Delhi and its vicinity: Implications for seismogenesis in the stable continental region of India," *Natural Hazards Research*, vol. 4, no. 3, pp. 448–458, Sep. 2024, doi: <https://10.1016/j.nhres.2023.11.003>.
- [24] H. J. Wattimanela and S. J. Latupeirissa, "Analysis of Tectonic Earthquake Characteristics in The Province of Nusa Tenggara Barat Indonesia and Its Surroundings," *J Phys Conf Ser*, vol. 1463, no. 1, p. 012002, Feb. 2020, doi: <https://10.1088/1742-6596/1463/1/012002>.
- [25] R. Manzo, S. Cesca, D. Galluzzo, M. La Rocca, M. Picozzi, and R. Di Maio, "Source analysis of low frequency seismicity at Mt. Vesuvius by a hybrid moment tensor inversion," *Journal of Volcanology and Geothermal Research*, vol. 454, p. 108173, Oct. 2024, doi: <https://10.1016/j.jvolgeores.2024.108173>.
- [26] J. Song *et al.*, "Moment tensor inversion of mining-induced seismic events and forward modeling of critical fault slip to prevent rockbursts," *Journal of Rock Mechanics and Geotechnical Engineering*, Jul. 2024, doi: <https://10.1016/j.jrmge.2024.07.001>.
- [27] S. Hara, Y. Fukahata, and Y. Iio, "P-wave first-motion polarity determination of waveform data in western Japan using deep learning," *Earth, Planets and Space*, vol. 71, no. 1, p. 127, Dec. 2019, doi: <https://10.1186/s40623-019-1111-x>.
- [28] C. Zhang, J. Zhang, and J. Zhang, "Deriving focal mechanism solutions of small to moderate earthquakes in Sichuan, China via a deep learning method," *Earthquake Research Advances*, p. 100371, Feb. 2025, doi: <https://10.1016/j.eqrea.2025.100371>.
- [29] R. Abdullah, "Analisis Seismisitas Berdasarkan Data Hasil Relokasi Hiposenter Gempabumi di Wilayah Ambarawa, Jawa Tengah," *Universitas Negeri Yogyakarta*, 2023.
- [30] P. Bormann, S. Wendt, and D. Di Giacomo, "Chapter 3 Seismic Sources and Source Parameters," 2013. doi: https://10.2312/GFZ.NMSOP-2_ch3.
- [31] T. Uchide, "Focal mechanisms of small earthquakes beneath the Japanese islands based on first-motion polarities picked using deep learning," *Geophys J Int*, vol. 223, no. 3, pp. 1658–1671, Sep. 2020, doi: <https://10.1093/gji/ggaa401>.
- [32] J. L. Hardebeck, "A New Method for Determining First-Motion Focal Mechanisms," *Bulletin of the Seismological Society of America*, vol. 92, no. 6, pp. 2264–2276, Aug. 2002, doi: <https://10.1785/0120010200>.
- [33] M. G. Ciaccio, R. Di Stefano, L. Improta, and M. T. Mariucci, "First-Motion Focal Mechanism

Solutions for 2015–2019 $M \geq 4.0$ Italian Earthquakes,” *Front Earth Sci (Lausanne)*, vol. 9, pp. 1–19, May 2021, doi: <https://10.3389/feart.2021.630116>.

- [34] M. Zhao, Z. Xiao, M. Zhang, Y. Yang, L. Tang, and S. Chen, “DiTingMotion: A deep-learning first-motion-polarity classifier and its application to focal mechanism inversion,” *Front Earth Sci (Lausanne)*, vol. 11, Mar. 2023, doi: <https://10.3389/feart.2023.1103914>.
- [35] A. Zollo, S. Nazeri, and S. Colombelli, “Earthquake Seismic Moment, Rupture Radius, and Stress Drop From P-Wave Displacement Amplitude Versus Time Curves,” *IEEE Transactions on Geoscience and Remote Sensing*, vol. 60, pp. 1–11, 2022, doi: <https://10.1109/TGRS.2021.3119909>.
- [36] J. Sileny, S. Cesca, and R. Hofstetter, “Single-Station Estimates of the Focal Mechanism for Weak Earthquakes,” *Seismological Research Letters*, vol. 94, no. 2A, pp. 944–960, Mar. 2023, doi: <https://10.1785/0220220096>.
- [37] T. King, S. Vinciguerra, J. Burgess, P. Benson, and L. De Siena, “Source Mechanisms of Laboratory Earthquakes During Fault Nucleation and Formation,” *J Geophys Res Solid Earth*, vol. 126, no. 5, May 2021, doi: <https://10.1029/2020JB021059>.
- [38] X. Jia, S. Li, Z. Liu, and C. Gong, “Normative expression and accurate understanding of focal mechanism parameters,” *Geosystems and Geoenvironment*, vol. 2, no. 2, p. 100154, May 2023, doi: <https://10.1016/j.geogeo.2022.100154>.
- [39] R. B. Herrmann, “A Student’s Guide to the Use of P and S Wave Data For Focal Mechanism Determination,” *Seismological Research Letters*, vol. 46, no. 4, pp. 29–39, Oct. 1975, doi: <https://10.1785/gssrl.46.4.29>.
- [40] V. Sharma *et al.*, “A long duration non-volcanic earthquake sequence in the stable continental region of India: The Palghar swarm,” *Tectonophysics*, vol. 779, p. 228376, Mar. 2020, doi: <https://10.1016/j.tecto.2020.228376>.
- [41] D. F. Yudiantoro *et al.*, “Geotourism of Telomoyo Volcano complex: an in-depth analysis for future development,” *IOP Conf Ser Earth Environ Sci*, vol. 1339, no. 1, p. 012032, May 2024, doi: <https://10.1088/1755-1315/1339/1/012032>.
- [42] S. Takemura *et al.*, “A review of shallow slow earthquakes along the Nankai Trough,” *Earth, Planets and Space*, vol. 75, no. 1, p. 164, Oct. 2023, doi: <https://10.1186/s40623-023-01920-6>.
- [43] L. De Barros, F. Cappa, A. Deschamps, and P. Dublanchet, “Imbricated Aseismic Slip and Fluid Diffusion Drive a Seismic Swarm in the Corinth Gulf, Greece,” *Geophys Res Lett*, vol. 47, no. 9, pp. 1–9, May 2020, doi: <https://10.1029/2020GL087142>.
- [44] H. Yang and S. Yao, “Shallow destructive earthquakes,” *Earthquake Science*, vol. 34, no. 1, pp. 15–23, Feb. 2021, doi: <https://10.29382/eqs-2020-0072>.
- [45] J. A. Power and D. C. Roman, “Event classification, seismicity, and eruption forecasting at Great Sitkin Volcano, Alaska: 1999–2023,” *Journal of Volcanology and Geothermal Research*, vol. 454, p. 108182, Oct. 2024, doi: <https://10.1016/j.jvolgeores.2024.108182>.
- [46] B. U. Bukit, “Integration Of 3G Data (Geomagnetic, Gravity And Geology) To Identify Geothermal System Controlled By Geological Structure Of Telomoyo Plateau (Study Case Of Candi Umbul Area),” *Journal of Petroleum and Geothermal Technology*, vol. 5, no. 1, p. 42, May 2024, doi: <https://10.31315/jpgt.v5i1.11929>.
- [47] H. U. Annisa, H. Niniek Rina, and D. Hermawan, “Fluid evolution of Umbul-Telomoyo Geothermal system,” in *IOP Conference Series: Earth and Environmental Science*, Institute of Physics Publishing, 2019. doi: <https://10.1088/1755-1315/254/1/012003>.
- [48] Y. Z. Abdillah *et al.*, “Geochemistry of Cold Springs in Geothermal Exploration Stage – Case Study

of Candi Umbul Telomoyo, Central Java,” in *IOP Conference Series: Earth and Environmental Science*, Institute of Physics, 2024. doi: <https://10.1088/1755-1315/1293/1/012004>.

- [49] G. Zhao *et al.*, “Inversion of the Temperature and Depth of Geothermal Reservoirs Using Controlled Source Audio Frequency Magnetotellurics and Hydrogeochemical Method,” *Front Earth Sci (Lausanne)*, vol. 10, May 2022, doi: <https://10.3389/feart.2022.858748>.
- [50] X. Bu, K. Jiang, and Y. He, “Performance analysis of shallow depth hydrothermal enhanced geothermal system for electricity generation,” *Geothermics*, vol. 86, p. 101847, Jul. 2020, doi: <https://10.1016/j.geothermics.2020.101847>.
- [51] T. M. Alves, N. H. Mattos, S. Newnes, and S. Goodall, “Analysis of a basement fault zone with geothermal potential in the Southern North Sea,” *Geothermics*, vol. 102, p. 102398, Jun. 2022, doi: <https://10.1016/j.geothermics.2022.102398>.
- [52] M. Zucchi, “Faults controlling geothermal fluid flow in low permeability rock volumes: An example from the exhumed geothermal system of eastern Elba Island (northern Tyrrhenian Sea, Italy),” *Geothermics*, vol. 85, p. 101765, May 2020, doi: <https://10.1016/j.geothermics.2019.101765>.
- [53] D. Sianipar, R. Sipayung, and E. Ulfiana, “Excessive seismicity over a limited source: the August 2019 earthquake swarm near Mt. Salak in West Java (Indonesia),” *J Seismol*, vol. 24, no. 6, pp. 1189–1204, Dec. 2020, doi: <https://10.1007/s10950-020-09957-w>.
- [54] T. M. Alves, N. H. Mattos, S. Newnes, and S. Goodall, “Analysis of a basement fault zone with geothermal potential in the Southern North Sea,” *Geothermics*, vol. 102, p. 102398, Jun. 2022, doi: <https://10.1016/j.geothermics.2022.102398>.
- [55] M. Zucchi, “Faults controlling geothermal fluid flow in low permeability rock volumes: An example from the exhumed geothermal system of eastern Elba Island (northern Tyrrhenian Sea, Italy),” *Geothermics*, vol. 85, p. 101765, May 2020, doi: <https://10.1016/j.geothermics.2019.101765>.
- [56] K. Sirorattanakul, Z. E. Ross, M. Khoshmanesh, E. S. Cochran, M. Acosta, and J. Avouac, “The 2020 Westmorland, California Earthquake Swarm as Aftershocks of a Slow Slip Event Sustained by Fluid Flow,” *J Geophys Res Solid Earth*, vol. 127, no. 11, pp. 1–35, Nov. 2022, doi: <https://10.1029/2022JB024693>.
- [57] Y. Yukutake, K. Yoshida, and R. Honda, “Interaction Between Aseismic Slip and Fluid Invasion in Earthquake Swarms Revealed by Dense Geodetic and Seismic Observations,” *J Geophys Res Solid Earth*, vol. 127, no. 4, pp. 1–18, Apr. 2022, doi: <https://10.1029/2021JB022933>.
- [58] A. D. Nugraha, P. Supendi, S. Widiyantoro, D. Daryono, and S. Wiyono, “Earthquake swarm analysis around Bekancan area, North Sumatra, Indonesia using the BMKG network data: Time periods of February 29, 2015 to July 10, 2017,” in *AIP conference proceedings*, AIP Publishing, 2018.
- [59] P. Supendi *et al.*, “Earthquake Swarm Analysis around Mt. Salak, West Java, Indonesia, Using BMKG Data from August 10 to November 24, 2019,” in *IOP Conference Series: Earth and Environmental Science*, IOP Publishing Ltd, Nov. 2021. doi: <https://10.1088/1755-1315/873/1/012002>.
- [60] D. Legrand, “Which earthquake can trigger a volcanic eruption?,” *Journal of Volcanology and Geothermal Research*, vol. 432, p. 107698, Dec. 2022, doi: <https://10.1016/j.jvolgeores.2022.107698>.